2019 IEEE 16th International Conference on Rehabilitation Robotics (ICORR)
Toronto, Canada, June 24-28, 2019

Hybrid Control Interface of a Semi-soft Assistive Glove for People with Spinal Cord Injuries*

Daisuke Kaneishi[1], Robert Peter Matthew[2], Jessica EnShiuan Leu[1], Julia O'Donnell[1], Bike Zhang[1], Masayoshi Tomizuka[1], and Hannah Stuart[1]

Abstract— **Active assistive devices have been designed to augment the hand grasping capabilities of individuals with spinal cord injuries (SCI). An intuitive bio-signal of wrist extension has been utilized in the device control, which imitates the passive grasping effect of tenodesis. However, controlling these devices in this manner limits the wrist joint motion while grasping. This paper presents a novel hybrid control interface and corresponding algorithms (i.e., a hybrid control method) of the Semi-soft Assistive Glove (SAG) developed for individuals with C6/C7-SCI. The secondary control interface is implemented to enable/disable the grasp trigger signal generated by the primary interface detecting the wrist extension. A simulation study reveals that the hybrid control method can facilitate grasping situations faced in daily activities. Empirical results with three healthy subjects suggest that the proposed method can assist the user to reach and grasp objects with the SAG naturally.**

I. INTRODUCTION

A. Background

It is known that damage to the spinal cord at C6 or C7 manifests as tetraplegia (quadriplegia), with loss of sensory and motor function including the hands and arms [1]. As grasping hand functionality is important for independence [2], a broad range of assistive technologies have been designed to augment the grasping capabilities of individuals with spinal cord injuries (SCI). Some of these popular technologies are assistive devices such as orthoses [3] and exoskeletons [4]. The control interfaces and corresponding algorithms are critical for these devices to assist the users' daily activities naturally. Note that we refer to "control interfaces and corresponding algorithms" as "control methods" in the following passages.

The control methods for active assistive devices have been studied and developed for several decades [5], [6]. They allow the user to interact with the assistive devices safely and smoothly. These methods detect the user's intention with signals *explicitly* or *implicitly* related to the motion intention [7], [8], [9], [10], [11]. An on-off control signal generated by a momentary push button *explicitly* reflects the user's intention to actuate a hand exoskeleton [7]. Accordingly, the button can significantly reduce unexpected activation and prevents the user from injuries.

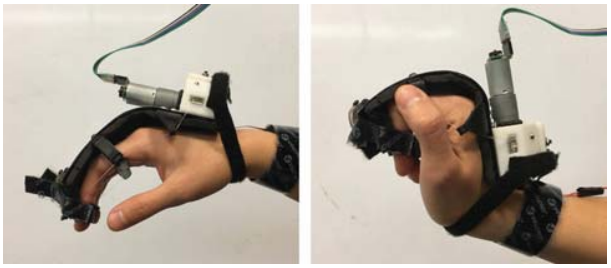

Fig. 1. Function of developed Semi-soft Assistive Glove (SAG). Wrist flexion is utilized to trigger the motor, imitating a tenodesis grasp [12].

On the other hand, selected bio-signals as interfaces with novel algorithms can be utilized to infer the user's intention *implicitly*. Humans are inherently familiar with coordinating muscle activation to generate joint motion. The implicit relation between muscular activation and limb movements may be exploited by retraining agonists of the movement or other muscles as a control interface through surface electromyography (sEMG) [8]. Yun et al. utilized sEMG with an artificial neural network (ANN) to detect the next grasp intent among three hand poses (transverse volar grip, lateral pinch, and extension grip) [9]. The ANN investigates the highly nonlinear relation between sEMG and the hand movements. This method could provide an intuitive functionality attractive with the user to control the device and may work well in rehabilitation facilities, as the algorithm (i.e., ANN) can be trained with enough data collected during rehabilitative training and/or exercise. Grasp misclassification may limit adoption of these technologies. Real-world grasp situations typically require a wide range of grasp types, beyond the three previously studied.

B. Related Work

Wrist extension is considered an intuitive and reliable bio-signal as an interface for individuals with C6/C7-SCI. These users are familiar with using this motion to achieve a weak passive grasp through tenodesis[1] without an orthosis [10]. The familiarity of the control motion could be useful for people with SCI. The relative joint movement can be measured reliably with sensors such as bending sensors

*This work was supported by Funai Foundation for Information Technology and University of California, Berkeley.

[1] Authors are with the Department of Mechanical Engineering, University of California, Berkeley, CA 94720, USA, {kaneishi, jess.leu24, julia_odonnell, bikezhang, tomizuka, hstuart} @berkeley.edu

[2] R.P. Matthew is with the Department of Electrical Engineering and Computer Science, University of California, Berkeley, CA 94720, USA, {rpmatthew} @berkeley.edu

[1]Tenodesis, the passive closing of the hand upon wrist extension and opening upon wrist flexion, is an established means for people with SCI to lightly grasp objects, and has been augmented with mechanical devices such as the *tenodesis hand splint*

Fig. 2. Object manipulation situations faced in daily activities such as grabbing a bottle and opening a door, demonstrated with a healthy individual. The hand is open in both reaching motions, but the wrist is more flexed (left) or extended (right) depending on orientation of objects.

and goniometers. With these sensors, the control via wrist extension can be realized by a simple algorithm (e.g., a threshold method [12]). However, this control method introduces some geometrical and dynamical constraints on the distal limbs. Figure 1 shows the function of the Semi-soft Assistive Glove (SAG) utilizing wrist extension as a control interface [12]. Because wrist motion is utilized as a trigger to assist grasping, the user cannot open the hand when the joint is extended (Figure 1, Right). This constraint may inhibit the user from grasping objects in the most natural orientations, or may force them to utilize compensatory movements. For example, the user is not able to contact the object without wrist extension in situations such as the case shown in Figure 2 (Right). The SAG then closes the user's hand before grasping the object. Thus, the control method with the singular interface of wrist motion may limit the user's activities.

C. Contribution

This paper introduces of a hybrid control method for active assistive devices related to SAG as shown in Figure 1 [12] and evaluates performances of the method both in theory and practice. The proposed hybrid control method uses two control interfaces. The primary control interface detects the user's wrist extension to assist grasping, as in our previous study [12]. The secondary interface enables the user to activate or deactivate the function of the primary interface to respond to several situations. A simple but effective algorithm for these hybrid interfaces is proposed based on a finite state machine.

A simulation study and experiments were conducted to validate performance of the proposed hybrid control methods. Section II shows the simulation study with an upper extremity model and two simplified grasping conditions. We numerically validated the necessity of the hybrid control method by indicating that the user cannot avoid compensatory movements in some situations using the previous method of singular interface. In Section III, we described the hybrid control method and human evaluations that were conducted with three healthy subjects with our prototype. Through these numerical and empirical studies, we confirmed that the proposed hybrid control method could improve the user's grasping performance with hand-assistive devices.

II. SIMULATION STUDY

In general, performances of control methods are difficult to evaluate in experiments when tied to the highly-complex human actuation system. The user could decide to grasp objects through any voluntary compensatory motions, or to grasp in a different way by changing the arrangement of the objects. Thus, we first analyzed the necessity of the hybrid control method by mathematically modeling the human grasp approach and actuation. The user was modeled as fixed torso with an upper extremity with seven degrees of freedom, and objects were simplified as target finger positions. We set constraints on the wrist joint angle corresponding to the defined control interface.

A. Conditions of Simulation

1) Upper Extremity Model: As shown in Figure 3, an upper extremity model is developed to validate performance of the proposed control method through a simulation study. Note that the user is assumed to wear the device on the right hand. The user is modeled sitting on a wheelchair with fixed torso position, as is common for an individual with C6/7-SCI. The model consists of three rigid bodies: an upper arm (l_u), a forearm (l_f), and a hand. There are seven degrees of freedom (DoF) $\boldsymbol{\theta} \in \mathbb{R}^7$ which correspond to each joint angle: shoulder rotation (θ_1), shoulder flexion (θ_2), shoulder abduction (θ_3), elbow flexion (θ_4), wrist rotation (θ_5), wrist radial flexion (θ_6), and wrist flexion (θ_7). These joint angles determine coordinates of the elbow and wrist joint center ($\boldsymbol{p}_{elb}$, $\boldsymbol{p}_{wri} \in \mathbb{R}^3$). Positions of thumb, index, and little finger ($\boldsymbol{p}_{thb}$, $\boldsymbol{p}_{idx}$, and $\boldsymbol{p}_{lit} \in \mathbb{R}^3$) are defined relative to the coordinate of wrist joint center, $\boldsymbol{p}_{wri}$ (Figure 4).

The following mathematical formulation utilizes relative coordinate frame transformations to relate these joint positions to corresponding joint angles in the model. World and local coordinate frames of the upper extremity model are shown in Figure 3 on the left limb. We defined identical local coordinate frames for the right limb, and we used the frames on the right in the simulation. Origins of each frame are located at the joint centers, and the Z axis is arranged along with the proximal body segments. The homogeneous transformation between the world and shoulder frame $\boldsymbol{g}_{w,sho}$ is thus formulated as:

$$\boldsymbol{g}_{w,sho}(\boldsymbol{p}_{sho}, \theta_1, \theta_2, \theta_3) = \begin{bmatrix} \boldsymbol{R}_Z(\theta_1)\boldsymbol{R}_Y(\theta_2)\boldsymbol{R}_X(\theta_3) & \boldsymbol{p}_{sho} \\ \boldsymbol{0}_{1\times 3} & 1 \end{bmatrix} \tag{1}$$

where $\boldsymbol{p}_{sho} \in \mathbb{R}^3$ is a coordinate of the shoulder joint center in the world frame, $\boldsymbol{R}_Z$, $\boldsymbol{R}_Y$, and $\boldsymbol{R}_X \in \mathbb{R}^{3\times 3}$ are the standard rotation matrices about the Z, Y, and X axes, respectively. Similarly, the relative transformations between shoulder and elbow frame $\boldsymbol{g}_{sho,elb}$ and elbow and wrist frame $\boldsymbol{g}_{elb,wri}$ can be written as:

$$\boldsymbol{g}_{sho,elb}(l_u, \theta_4) = \begin{bmatrix} \boldsymbol{R}_Y(\theta_4) & \begin{bmatrix} 0 \\ 0 \\ -l_u \end{bmatrix} \\ \boldsymbol{0}_{1\times 3} & 1 \end{bmatrix} \tag{2}$$

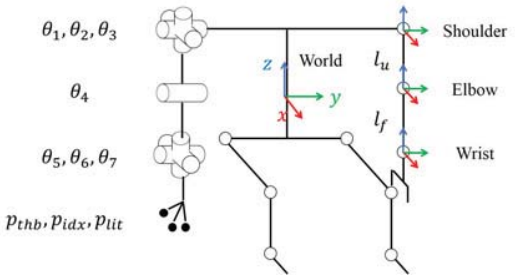

Fig. 3. Upper extremity model as a rigid-link model with 7 degrees of freedom. Finger positions relative to the wrist joint center are described in Figure 4.

$$\boldsymbol{g}_{elb,wri}(l_f,\theta_5,\theta_6,\theta_7) = \begin{bmatrix} \boldsymbol{R}_Z(\theta_5)\boldsymbol{R}_Y(\theta_6)\boldsymbol{R}_X(\theta_7) & \begin{bmatrix} 0 \\ 0 \\ -l_f \end{bmatrix} \\ \boldsymbol{0}_{1\times 3} & 1 \end{bmatrix} \tag{3}$$

These homogeneous transformations (1) to (3) are used to compute the world frame coordinates of the finger positions from their local positions $\boldsymbol{P}_{hand}$ such as:

$$\begin{bmatrix} \boldsymbol{p}_{thb} & \boldsymbol{p}_{idx} & \boldsymbol{p}_{lit} \\ 1 & 1 & 1 \end{bmatrix} = \boldsymbol{g}_{w,sho}\boldsymbol{g}_{sho,elb}\boldsymbol{g}_{elb,wri}\boldsymbol{P}_{hand} \tag{4}$$

$$\boldsymbol{P}_{hand} = \begin{bmatrix} x_h & x_h & x_h - 0.05 \\ y_h & y_h & y_h \\ z_h & z_h - 0.05 & z_h - 0.05 \\ 1 & 1 & 1 \end{bmatrix} \tag{5}$$

where the matrix $\boldsymbol{P}_{hand}$ is determined based on the model in Figure 4.

2) Object Model: We specified the desired finger positions for the thumb, index, and little finger instead of the geometry of multiple objects, assuming that the user can grasp the object if they reach the target positions. The desired finger positions for the grasping $\boldsymbol{p}_{d,i} \in \mathbb{R}^3$ are defined as follows:

$$\boldsymbol{p}_{d,i} = [p_{x_d,i}, p_{y_d,i}, p_{z_d,i}]^T \tag{6}$$

where $i \in \{thb, idx, lit\}$, and $p_{x_d,i}, p_{y_d,i}, p_{z_d,i} \in \mathbb{R}$ are coordinates in Cartesian space. In this study, the desired finger positions are defined simply on either the sagittal (z-x) or frontal (y-z) planes as shown in Figure 5(i). For example, if the user sits on the wheelchair fixed in front of a door, the user is forced to approach a doorknob from the direction nearly normal to the frontal plane (i.e., x axis). Thus, a doorknob can be modeled with the desired finger positions on the frontal plane as shown in Figure 5(ii).

3) Wrist Postures for Analysis: When the singular control interface is implemented on an assistive device, it demands the user extend their joint to close their hand, and vice versa. It can be modeled that the user with the singular control interface is limited to approach in a wrist posture A, defined by wrist flexion $\theta_7 = 0$, as shown in Figure 4A. Note that the wrist posture B with $\theta_7 = -\pi/2$ (Figure 4B) can be achieved only when the singular control interface is deactivated.

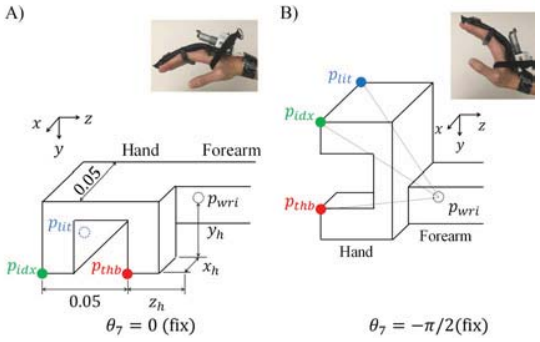

Fig. 4. A) Relaxed ($\theta_7 = 0$) and B) extended ($\theta_7 = -\pi/2$) wrist posture without active assistance. Schematic diagrams describe hand models for each posture.

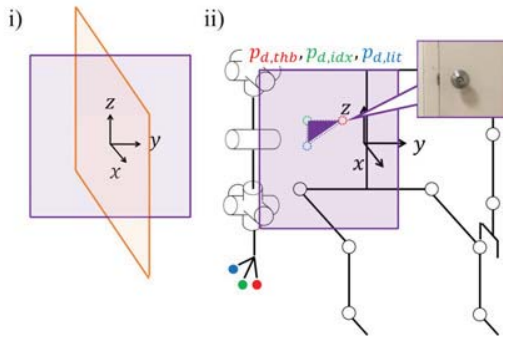

Fig. 5. i) Definition of a sagittal (z-x, orange) and frontal (y-z, purple) planes in this paper. ii) Desired finger positions to grasp a doorknob modeled for the upper extremity model in Figure 3.

4) Grasping Performance Index: To successfully grasp an object modeled as the desired positions, we assume that the user's finger positions must be aligned with the desired positions. Thus, the grasping performance in the two wrist postures can be analyzed quantitatively with the index J defined as follows:

$$\min_{\boldsymbol{\theta}} \quad J(\boldsymbol{\theta}) = \sum_i \|\boldsymbol{p}_{d,i} - \boldsymbol{p}_i\|_2 \tag{7a}$$

$$\text{s.t.} \begin{cases} \boldsymbol{p}_i = \boldsymbol{G}_1(\boldsymbol{\theta}, \boldsymbol{P}_{hand}) & (7b) \\ \underline{\boldsymbol{\theta}} \le \boldsymbol{\theta} \le \overline{\boldsymbol{\theta}} & (7c) \\ \theta_7 = \boldsymbol{G}_2(c) & (7d) \end{cases}$$

where $\underline{\boldsymbol{\theta}}$, $\overline{\boldsymbol{\theta}} \in \mathbb{R}^7$ are the lower and upper limits of the angles, $\boldsymbol{G}_1$ is a function which can be derived from (4), $c \in \{A, B\}$ suggests a condition of the wrist postures, and $\boldsymbol{G}_2$ is a function that assigns θ_7 to be either 0 or $-\pi/2$, according to the input c. To solve the nonlinear optimization problem (7), we computed gradients of the function (7a) with respect to $\boldsymbol{\theta}$ such that:

$$\frac{\partial J}{\partial \boldsymbol{\theta}} = \sum_i -2(\boldsymbol{p}_{d,i} - \boldsymbol{p}_i)\frac{\partial \boldsymbol{p}_i}{\partial \boldsymbol{\theta}} \tag{8}$$

The gradients in (8) for each i can be derived from (4). The optimization problem was solved in `MATLAB 2016b` installed in a laptop (Intel Core i-5, RAM 8GB). First, the finger positions $\boldsymbol{p}_i$ and the gradients for each i were

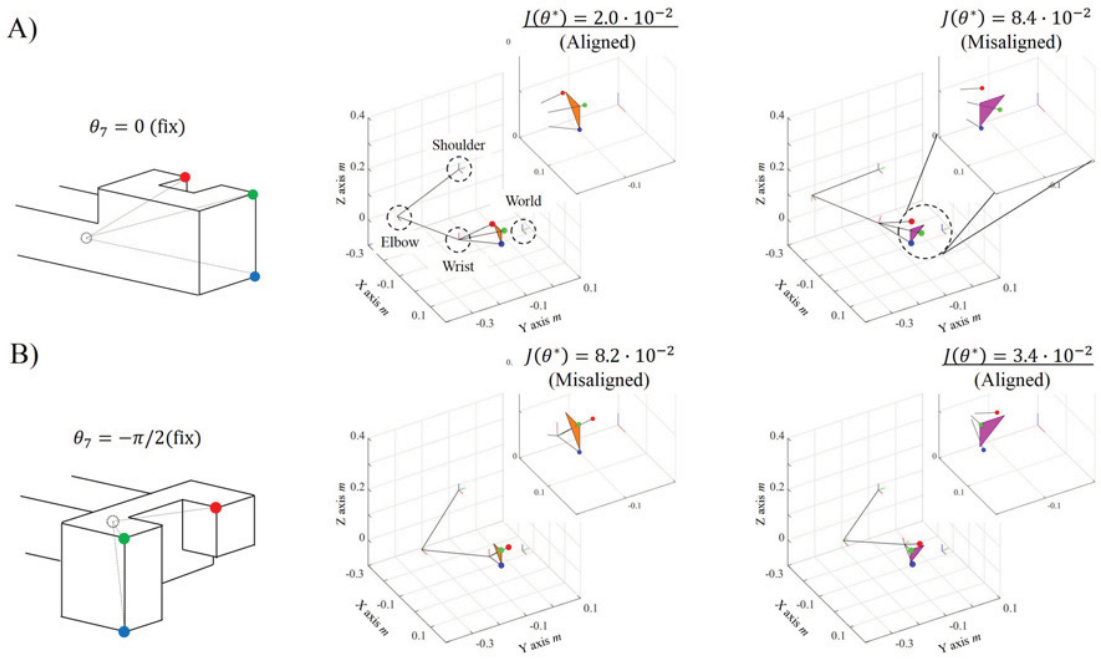

Fig. 6. Upper extremity models and corresponding grasping performance indexes J as simulation results of reaching to the desired finger positions in a sagittal (z-x, orange) and frontal (y-z, purple) planes with wrist postures A ($\theta_7 = 0$) and B ($\theta_7 = -\frac{\pi}{2}$) shown in Figure 4.

TABLE I
GRASPING PERFORMANCE INDEX $J(\boldsymbol{\theta}^*)$

		Desired Finger Positions	
		Sagittal	Frontal
Wrist Posture	A (θ_7 = 0)	$2.0 \cdot 10^{-2}$	$8.4 \cdot 10^{-2}$
	B (θ_7 = -π/2)	$8.2 \cdot 10^{-2}$	$3.4 \cdot 10^{-2}$

computed based on given $\boldsymbol{\theta}$ and the forward kinematics in (4). Then the gradients (8) were calculated with these results. `MATLAB fmincon` solver (internal point method) was used to numerically solve the optimization problem (7) based on the computed gradients. Initial values for the two conditions corresponding to wrist postures A and B were set as follows:

$$\boldsymbol{\theta}_0 = [0.01 \cdot \mathbf{1}^T \ 0]^T \quad (9)$$

$$\boldsymbol{\theta}_0 = [0.01 \cdot \mathbf{1}^T \ -\pi/2]^T \quad (10)$$

where $\mathbf{1}$ is a 6×1 vector having 1 in all the elements. Other parameters used in the simulation are described in APPENDIX.

B. Simulation Results

Table I summarizes grasping performance indices computed by (7a) under the optimal joint angles $\boldsymbol{\theta}^*$ for each condition. Figure 6 shows qualitative simulation results of the desired finger positions located on the sagittal and frontal plane, corresponding to the hand poses shown in Figure 4A and B. Each figure includes the world, shoulder, elbow, and wrist frame, and those X, Y, and Z axes are expressed in segments colored in red, green, and blue, respectively, following Figure 3. The black lines connecting those frames indicate an upper limb, a forearm, and a hand. In this paper, we expected that the desired and computed finger positions were *aligned* when all the fingers reach within $2.0 \cdot 10^{-2}$ m (i.e., $J \leq 6.0 \cdot 10^{-2}$) from their desired positions.

C. Discussion based on Simulation Results

Two different wrist postures (Figure 4A and B) were investigated numerically in terms of the grasping performance index J. The index suggests how closely the fingers can approach the desired positions. Table I and Figure 6 shows the results of the simulation study. With the wrist posture A, the index is smaller when the desired finger positions are located on the sagittal plane compared to the frontal plane. It can be confirmed in Figure 6A that the three RGB circles in the figure are aligned with the desired positions (i.e., colored, triangular plane in Figure 6A) if the grasping performance index J is small, and vice versa. Similarly, the index becomes small with the wrist posture B when the desired finger positions are located on the frontal plane (Table I). These results suggest that a user could grasp objects such as a bottle/doorknob naturally with the wrist posture A/B, respectively.

This simulation study suggests that a hybrid control method is important for the assistive device. The user is not able to grasp objects with the wrist posture B if the assistive device has the singular interface, because the device closes the user's hand before grasping the object. To grasp a doorknob, the user needs to perform compensatory movements such as twisting the upper body. In other words, the fixed $\boldsymbol{p}_{sho}$ in this simulation study needs to be modified to reduce the grasping performance index J.

It is thus reasonable to design a new control method which enables the user to grasp objects with the wrist posture A

and B. Thus, we introduce a hybrid control method, which utilizes the secondary interface to activate or deactivate the function of the primary interface to respond to both situations.

III. EMPIRICAL STUDY

A. Finite State Machine for Hybrid Control Interface

The overview of the proposed control scheme is shown in Figure 7 in the form of a finite state machine (FSM). When the hybrid control interfaces are implemented in an active assistive device, functions of the interface must be combined appropriately. Note the expansion from the previous single FSM F_2 [12]: F_2 is connected to a new FSM F_1 in series to augment performance of the device.

F_2 mimics tenodesis to activate an actuator by tracking the wrist motion, closing the hand upon wrist extension and opening upon wrist flexion. The binary signal *sig2* is thus designed as a guard condition based on wrist joint angle. Inputs θ_m and $\dot{\theta}_m$ are motor angle and angular velocity, implemented as safety limits to protect the user from injury and the motor from stall.

F_1 outputs its internal state as the last input signal *State* to F_2. When the device is turned on, F_1 is initially in the Functional state. F_2 will thus control the device to switch among the four states according to *sig*2. Upon receiving the input signal *sig*1, F_1 transits to Deactivated state, and correspondingly the state in F_2 transits to Neutral via Open state to open and maintain the hand pose. In the other words, F_1 switches states to deactivate the primary control interface which detects the wrist motion. F_1 remains in the Deactivated state, until *sig*1 is again detected and F_1 transits back to Functional state. Note that *sig*1 is a pure signal, which can be generated mechanically with a device such as a momentary switch.

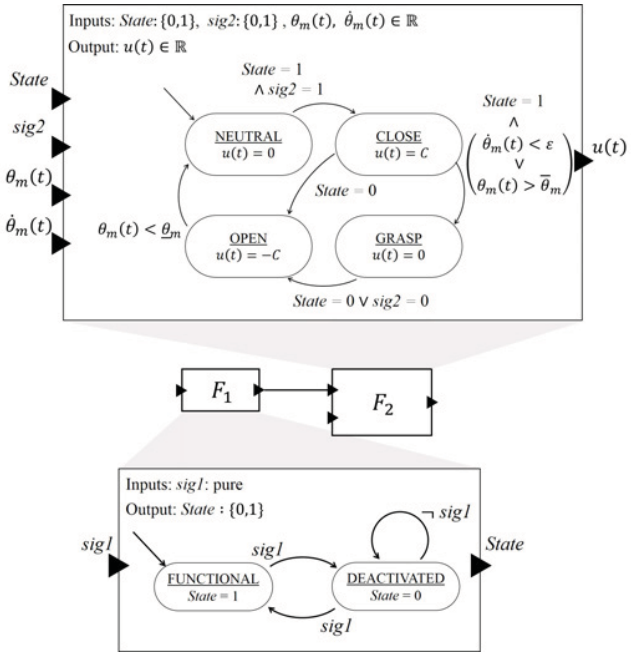

Fig. 7. Augmented hybrid control finite state machine (FSM) for Semi-soft Assistive Glove (SAG).

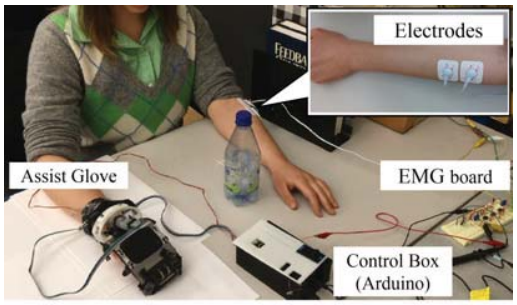

Fig. 8. Overview of human validation test setup.

B. Setup for Empirical Validation

Figure 8 shows an overview of the human validation test setup. Each subject wore the Semi-soft Assistive Glove (SAG) and a bend sensor on their right arm, and they attached sEMG electrodes on the left forearm. In this test, we evaluated performance of the hybrid control method in Figure 7 using the SAG [12]. The SAG consists of a leaf spring with an underactuated cable driven closing mechanism. The SAG can passively extend the user's fingers via the stiffness of the leaf spring, and it actively closes the user's hand by winding the cable with the geared motor.

We utilized a bend sensor (Adafruit, 1070) for the primary control interface as in our prior work [12]. The sensor was attached to the user's wrist to detect the wrist joint motion. Based on this sensor, a binary signal *sig*2 is designed as follows:

$$sig = \begin{cases} 0, & y(t) < \underline{\eta} \\ 1, & y(t) > \overline{\eta} \end{cases} \tag{11}$$

where $y(t)$ is the measured sensory data, and $\underline{\eta}$, $\overline{\eta} \in \mathbb{R}$ are constants tuned for each user. Through the hysteresis control method of setting $\underline{\eta} < \overline{\eta}$, the controller can avoid unintentional chattering effects. This binary signal *sig*2 is designed as a guard condition to turn on the actuator, i.e., switching from Neutral to Close state or from Grasp to Open state (Figure 7).

A sEMG sensor was utilized as the secondary control interface. The function of this sensor is to generate a pure signal *sig*1 in F_1 as shown in Figure 7. Thus, we could avoid using classifiers with machine learning techniques (e.g., ANN [9]) to collect training data. Instead, we binarized the sEMG signal to extract *sig*1 using the same hysteresis threshold method as for the bend sensor. We attached electrodes (2560 Red Dot Multi-Purpose Monitoring Electrode, 3M) at the user's extensor carpi radialis muscle to detect the wrist extension of the left arm. These electrodes can be attached to the right arm, and their locations may be optimized for the grasping motion through biomechanical analysis with a musculoskeletal simulator [13]. While this method may require more training to coordinate, it would allow for control of the orthosis with a single limb. However, the scope of the human validation tests described in this

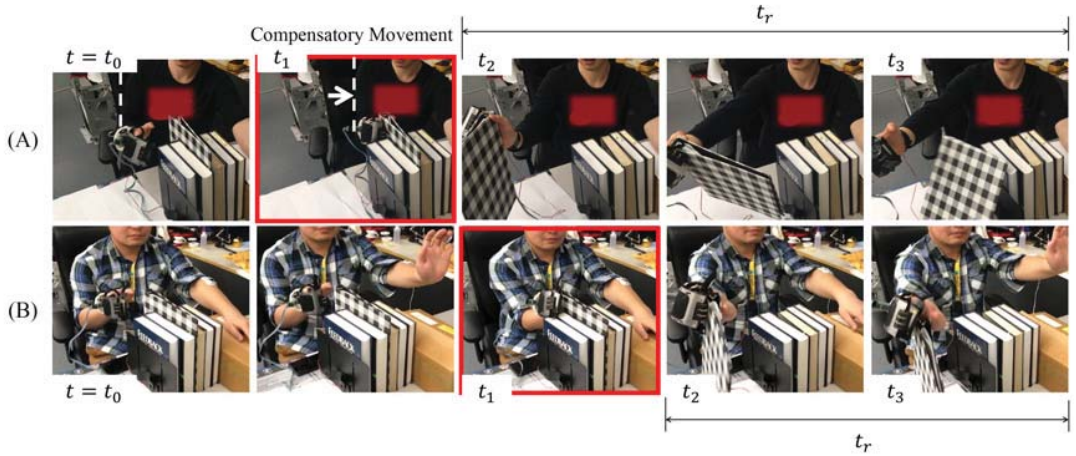

Fig. 9. A sequence of motions to grasp a plaid binder, A) in a wrist posture *A* with the singular control method and B) in a wrist posture *B* with the hybrid control method. Time stamps (e.g., t_0) are described in Section III-D.

paper is to evaluate performances of the hybrid control method. Thus, we determined to use the other arm motion as a trigger, as the motion does not influence the simulation conditions and does not confuse the subjects during testing.

A custom voltage amplifier (EMG board in Figure 8) was developed to measure sEMG from electrodes, and the amplified gain of the circuit is tuned manually for each individual. The circuit also has a function to produce offset voltage at 2.5 V. All the sensor values were measured with a microcontroller (Arduino UNO) in a control box (Figure 8). The raw bend sensor value was processed by moving average ($n = 10$), and the raw sEMG signal was average-rectified and processed by moving average ($n = 25$). Based on these processed signals and our control algorithm, the microcontroller controls the geared motor mounted on the glove to assist the user.

C. Human Validation Test Conditions

Three healthy individuals (2 males, 1 female, all right handed) were recruited under informed consent, which was approved by the Institutional Review Board of University of California, Berkeley (IRB: 2012-12-4872). In this study, subjects were asked to grasp two objects using the SAG with both the singular and the hybrid control interface. The subject was informed about functions of the glove and donned all the experimental apparatus. Then they had a few minutes to get familiar with the device. Subjects were asked not to use their own grip strength for grasping.

Two objects were determined to imitate grasping conditions applied in the simulation study. The first object was chosen to be a bottle because subjects often approached the objects from the direction normal to the sagittal plane in the previous study [12]. The other object was a binder arranged in a bookshelf, as we assume that the subjects need to approach to the binder from the direction along the x-axis as modeled in Figure 5(ii).

Two trials were conducted for each object. In the first trial, the subjects were asked to only utilize the singular control interface (i.e., a bend sensor on a wrist) to trigger the actuator. In the second trial, the subjects were allowed to use the hybrid control interfaces. All the trials were video recorded.

D. Test Results

Figure 9 shows a sequence of motions confirmed during grasping the plaid binder. A supplemental video provides the case of grasping the bottle. In Figure 9, we defined each time stamp t_0 to t_3 based on the subjects' actions. The subjects started to move at t_0, and we defined t_1 when an object was lifted up with the assistive glove. t_2 was determined when the subjects began to open the glove using the control interface. Finally, the object dropped onto the table at time t_3. With these time variables t_0 to t_3, another time stamp, the release time t_r, was computed as follows:

$$t_r = t_3 - t_2 \tag{12}$$

Figure 9A shows the first trial utilizing only a bend sensor, with time duration $t_r = 17.9$ seconds. Figure 9B shows the second trial utilizing the hybrid control method (i.e., both a bend sensor and sEMG sensor), with time duration $t_r = 1.0$ seconds.

E. Discussion based on Human Validation Test Results

We confirmed performance of the hybrid control method in the experiences under the same conditions as the simulation study. Figure 9 shows a sequence of motions to grasp a plaid binder. It was difficult for subjects to approach the binder from the side or top (i.e., sagittal or transverse plane) naturally due to other books and the subjects' seated height. Thus, we assume that the desired finger positions for grasping the binder could be modeled on the frontal plane like a doorknob in Figure 5, similar to one of the simulation conditions.

The simulation results suggest that the singular control interface, which allows only the wrist position *A*, may force the subjects to behave unnaturally (i.e., perform compensatory movements) in this situation. Figure 9A shows the human test results with the singular control method. The

subject could successfully grasp the binder with the SAG and moved it to the side. However, comparing postures of the subject at time t_1 with t_0, the subject showed a compensatory movement of the body not to trigger the device by the wrist extension. On the other hand, Figure 9B shows the case that the subject utilized the secondary interface (i.e., a sEMG sensor) to approach in the wrist posture *B*. There was nearly no difference at time t_1 and t_0 in the subject's posture according to the figures, which corresponds to the high grasping performance index confirmed in the simulation study.

According to these connections between theoretical and human validation test results discussed in Section II and III, we may conclude that the proposed hybrid control method is important to the assistive device for daily activities as it enables the user to achieve grasping more naturally.

A further benefit to the hybrid control method is that the additional interface provides the user with more input options to open the hand, which can result in smoother opening as well as closing. The singular-control test subject in Figure 9A spent some time ($t_r = 17.9$ seconds) to open the glove and drop the binder by flexing the wrist. However, by utilizing the secondary control interface (i.e., a sEMG sensor) as shown in Figure 9B, the subject could smoothly ($t_r = 1.0$ seconds) drop the object. We expect this effect to be most pronounced when handling large or bulky objects that are more difficult to move.

F. Limitation and Future Work

We identified that there are several limitations in this study. First, the kinematic simulation study in Section II was conducted with an upper extremity model in two simplified conditions. A kinetic simulation including a torso model may provide more precise analysis to explain our empirical results and to design an improved control interface.

Second, the performance was evaluated in practice with a limited number of healthy subjects utilizing video records. Future work is necessary to confirm performance of the proposed control interface with individuals with SCI using a motion capture system for more quantitative analysis.

IV. CONCLUSION

This paper presents a hybrid control method for assistive devices related to a Semi-soft Assistive Glove (SAG). Simulation study suggests that the secondary interface is important to facilitate grasping situations faced in daily activities. Along with the simulation study, human validation tests were conducted with three healthy subjects. We implemented a bend sensor and an sEMG sensor as the hybrid control interfaces. The control algorithm designed with the finite state machine (FSM) was implemented to combine the functions. These empirical results suggested that the proposed hybrid method could help the user to grasp objects more naturally. Future work will evaluate its performance with individuals with SCI using more robust measurement systems.

ACKNOWLEDGMENT

The authors would like to thank to Campbell Affleck, Andrew McPherson, Monica Li, and Kim Euiyoung for helpful conversations on theoretical and specific design concepts.

APPENDIX

The following Table shows parameters used in Section II.

Variable [unit]	Value	Variable [unit]	Value
l_u $[m]$	$2.50 \cdot 10^{-1}$	l_f $[m]$	$2.50 \cdot 10^{-1}$
$p_{x_{sho}}$ $[m]$	$-1.50 \cdot 10^{-1}$	$p_{y_{sho}}$ $[m]$	$-1.50 \cdot 10^{-1}$
$p_{z_{sho}}$ $[m]$	$2.00 \cdot 10^{-1}$	x_h $[m]$	$5.00 \cdot 10^{-2}$
y_h $[m]$	$1.00 \cdot 10^{-1}$	z_h $[m]$	$5.00 \cdot 10^{-2}$
$\overline{\theta_1}$ $[rad]$	$\pi/2 - 0.01$	$\underline{\theta_1}$ $[rad]$	0.0
$\overline{\theta_2}$ $[rad]$	$\pi/6$	$\underline{\theta_2}$ $[rad]$	$-5\pi/6$
$\overline{\theta_3}$ $[rad]$	0.0	$\underline{\theta_3}$ $[rad]$	$-\pi/2 + 0.01$
$\overline{\theta_4}$ $[rad]$	0.0	$\underline{\theta_4}$ $[rad]$	$-5\pi/6$
$\overline{\theta_5}$ $[rad]$	$\pi/2 - 0.01$	$\underline{\theta_5}$ $[rad]$	$-\pi/2 + 0.01$
$\overline{\theta_6}$ $[rad]$	$\pi/6$	$\underline{\theta_6}$ $[rad]$	$-\pi/12$

REFERENCES

[1] L. Harvey, J. Batty, R. Jones, and J. Crosbie, "Hand function of c6 and c7 tetraplegics 1-16 years following injury," *Spinal Cord*, vol. 39, no. 1, pp. 37–43, 2001.

[2] G. Snoek, M. Ijzerman, H. J. Hermens, D. Maxwell, and F. Biering-Sorensen, "Survey of the needs of patients with spinal cord injury: impact and priority for improvement in hand function in tetraplegics," *Spinal Cord*, vol. 42, no. 9, pp. 526–532, 2004.

[3] S. Ates, C. J. W. Haarman, and A. H. A. Stienen, "Script passive orthosis: design of interactive hand and wrist exoskeleton for rehabilitation at home after stroke," *Autonomous Robots*, vol. 41, no. 3, pp. 711–723, 2017.

[4] P. Agarwal, Y. Yun, J. Fox, K. Madden, and A. D. Deshpande, "Design, control, and testing of a thumb exoskeleton with series elastic actuation," *The Int. J. of Robotics Research*, vol. 36, no. 3, pp. 355–375, 2017.

[5] D. S. Childress, "Powered limb prostheses: Their clinical significance," *IEEE Trans. on Biomedical Eng.*, vol. 20, no. 3, pp. 200–207, May 1973.

[6] J. Lobo-Prat, P. N. Kooren, A. H. Stienen, J. L. Herder, B. F. Koopman, and P. H. Veltink, "Non-invasive control interfaces for intention detection in active movement-assistive devices," *J. of Neuro-Engineering and Rehabilitation*, vol. 11, no. 1, p. 168, Dec 2014.

[7] B. W. Gasser, D. A. Bennett, C. M. Durrough, and M. Goldfarb, "Design and preliminary assessment of vanderbilt hand exoskeleton," in *Proc. IEEE Int. Conf. on Rehabilitation Robotics (ICORR)*, July 2017, pp. 1537–1542.

[8] D. Kaneishi, R. P. Matthew, and M. Tomizuka, "A sEMG classification framework with less training data," in *Proc. Int. Conf. of the IEEE Engineering in Medicine and Biology Society (EMBC)*, July 2018, pp. 1680–1684.

[9] Y. Yun, S. Dancausse, P. Esmatloo, A. Serrato, C. A. Merring, P. Agarwal, and A. D. Deshpande, "Maestro: An emg-driven assistive hand exoskeleton for spinal cord injury patients," in *Proc. IEEE Int. Conf. on Robotics and Automation (ICRA)*, May 2017, pp. 2904–2910.

[10] H. In, B. B. Kang, M. Sin, and K.-J. Cho, "Exo-glove: a wearable robot for the hand with a soft tendon routing system," *IEEE Robotics & Automation Magazine*, vol. 22, no. 1, pp. 97–105, 2015.

[11] D. Kim, B. B. Kang, K. B. Kim, H. Choi, J. Ha, K.-J. Cho, and S. Jo, "Eyes are faster than hands: A soft wearable robot learns user intention from the egocentric view," *Science Robotics*, vol. 4, no. 26, 2019.

[12] D. Kaneishi, J. E. Leu, J. ODonnell, C. Affleck, R. P. Matthew, A. McPherson, M. Tomizuka, and H. Stuart, "Design and preliminary assessment of a semi-soft assistive glove for people with spinal cord injuries," in *Proc. IEEE/RSJ Int. Conf. on Intelligent Robots and Systems (IROS), submitted*, Nov 2019.

[13] S. L. Delp, F. C. Anderson, A. S. Arnold, P. Loan, A. Habib, C. T. John, E. Guendelman, and D. G. Thelen, "Opensim: Open-source software to create and analyze dynamic simulations of movement," *IEEE Trans. on Biomedical Eng.*, vol. 54, no. 11, pp. 1940–1950, Nov 2007.